Available online at www.sciencedirect.com

SCIENCE DIRECT®

Journal of Solid State Chemistry 177 (2004) 4175–4182

JOURNAL OF SOLID STATE CHEMISTRY

www.elsevier.com/locate/jssc

Synthesis, crystal structure and optical properties of $BiMgVO_5$

S. Benmokhtar[a], A. El Jazouli[a,*], J.P. Chaminade[b], P. Gravereau[b], F. Guillen[b], D. de Waal[c]

[a] *LCMS, UFR Sciences des Matériaux Solides, Faculté des Sciences Ben M'Sik, UH2M, Casablanca B.P. 7955, Morocco*
[b] *Institut de Chimie de la Matière Condensée de Bordeaux (ICMCB-CNRS), Pessac 33608, France*
[c] *Department of Chemistry, University of Pretoria, Pretoria 0002, South Africa*

Received 12 November 2003; received in revised form 31 May 2004; accepted 7 June 2004

Abstract

The new vanadate $BiMgVO_5$ has been prepared and its structure has been determined by single crystal X-ray diffraction: space group $P2_1/n$, $a = 7.542(6)$ Å, $b = 11.615(5)$ Å, $c = 5.305(3)$ Å, $\beta = 107.38(5)°$, $wR_2 = 0.0447$, $R = 0.0255$. The structure consists of $[Mg_2O_{10}]$ and $[Bi_2O_{10}]$ dimers sharing their corners with $[VO_4]$ tetrahedra. The ranges of bond lengths are 2.129–2.814 Å for Bi–O; 2.035–2.167 Å for Mg–O and 1.684–1.745 Å for V–O. V–O bond lengths determined from Raman band wavenumbers are between 1.679 and 1.747 Å. An emission band overlapping the entire visible region with a maximum around 650 nm is observed.

Keywords: $BiMgOVO_4$; Oxyvanadate; Crystal structure; Raman; Optical properties

1. Introduction

Compounds containing vanadium and bismuth are of interest in many fields: oxygen ion conductors, bright yellow pigments, selective oxidation, catalysts [1–3]. Studies of Bi_2O_3–MO–X_2O_5 (M = Mg, Mn, Co, Ni; X = P, V, As) systems revealed the series of compounds as BiMXO_5. Crystal structures of BiMPO_5 (M = Mn, Co, Ni) [4–8], BiMVO_5 (M = Ca, Mn, Cd, Pb) [9–12] and $BiMnAsO_5$ [10] have been determined. To our knowledge the composition $BiMgVO_5$ has not been reported. Its powder and single crystal synthesis, crystal structure, vibrational spectra and optical properties are described here.

2. Experimental

Powder of $BiMgVO_5$ was prepared by solid-state reaction from a stoichiometric mixture of Bi_2O_3 (99%, Aldrich), MgO (98%, Merck) and NH_4VO_3 (99%, Merck). The mixture was heated at 200 °C, 500 °C and finally at 850 °C for 18 h with intermediate grinding. The obtained powder is yellow. Single crystals were prepared by melting the powder at 950 °C ± 20 °C and slow cooling in a platinum crucible. The sample was held at 950 °C for 15 min, cooled to 500 °C at rate of 3°C/h and finally cooled to room temperature by turning off the furnace power. Clear light yellow crystals corresponding to the formula $BiMgVO_5$ were obtained.

X-ray powder diffraction (XRPD) spectra were recorded at room temperature by using a Philips PW 3040 ($\theta - \theta$) diffractometer (Cu$K\alpha$ radiation, $\lambda = 1.5406$ Å). Single crystal X-ray diffraction data were obtained on an Enraf-Nonius CAD-4 automated diffractometer with graphite monochromator (Mo$K\alpha$ radiation, $\lambda = 0.71073$ Å) operating at 40 kV and 30 mA.

The Raman spectrum was recorded under the microscope of a Dilor XY Multichannel spectrometer. Excitation was accomplished with the 514.5 nm line of an argon-ion laser. Incident power was approximately 100 mW at the source, and 10% of that at the sample. The infrared spectra were recorded using a Bruker IFS

*Corresponding author. Fax: +212-22704675.
E-mail address: a.eljazouli@univh2m.ac.ma (A. El Jazouli).

0022-4596/$ - see front matter
doi:10.1016/j.jssc.2004.06.030

113 vs. FT-IR spectrometer. Samples were in the form of KBr (mid-IR) and polyethylene (far-IR) pellets.

The diffuse reflectance spectra were recorded at 300 K between 210 and 2400 nm using a double monochromator Cary 2400 spectrometer. Excitation and emission spectra have been recorded at 7 and 292 K using a SPEX FL 212 fluorimeter equipped with a SMC liquid helium cryostat. The excitation source was a high-pressure xenon emitting between 200 and 1000 nm.

3. Results and discussion

3.1. XRPD pattern analysis

XRPD pattern of $BiMgVO_5$ (Fig. 1) is close to that of $BiNiPO_5$ [4]. The crystal structure of the phosphate has been determined in the monoclinic system with $P2_1/n$ space group. A monoclinic unit cell was obtained, for $BiMgVO_5$, from single crystal X-ray diffraction experiments, carried out on an Enraf-Nonius CAD-4 diffractometer using Mo$K\alpha$ radiation, with $a = 7.542$ Å, $b = 11.615$ Å, $c = 5.305$ Å, $\beta = 107.38°$ $(Z = 4)$, $V = 443.5$ Å^3. Main data collection parameters of single crystal are summarized in Table 1. The corresponding cell parameters obtained from the XRPD pattern (Fig. 1; Table 2) are: $a' = 7.5439(7)$ Å, $b' = 11.615(2)$ Å, $c' = 5.3017(7)$ Å, $\beta' = 107.35(1)°$, $V = 443.4$ Å^3. We have chosen $P2_1/n$ as space group in spite of standard group $P2_1/c$ in order to compare with the previously determined phosphate structure $BiNiPO_5$ [4]. There is a similarity between these parameters and those of BiMPO$_5$ (M = Ni, Co, Mn); $a = 7.1664(8)$ Å, $b = 11.206(1)$ Å, $c = 5.1732(6)$ Å, $\beta = 107.281(6)°$ for $BiNiPO_5$, as example [4–8]. The high values observed for the vanadate are due to the size of V^{5+} (0.31 Å) greater than that of P^{5+} (0.17 Å) [13].

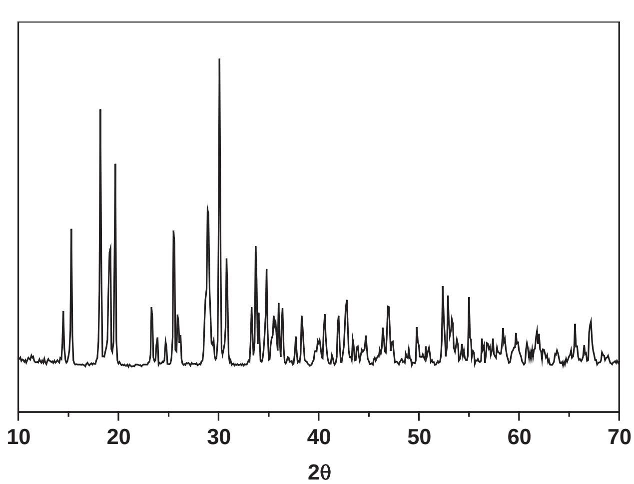

Fig. 1. X-ray diffraction pattern of the $BiMgVO_5$ powder.

Table 1
Crystal data and structure refinement for $BiMgVO_5$

Formula	$BiMgVO_5$
Formula weight (g/mol)	364.25
Temperature (K)	293(2)
Wavelength (Å)	0.71073
Crystal system	Monoclinic
Space group	$P2_1/n$
a (Å)	7.542(6)
b (Å)	11.615(5)
c (Å)	5.305(3)
β (deg)	107.38(5)°
Volume (Å^3)	443.5(5)
Z	4
Calculated density (g/cm^3)	5.455
Crystal size (μm)	60 × 100 × 280
Color	Light yellow
Diffractometer	CAD–4
Scan method	$\omega - 2\theta$
Absorption coefficient (mm^{-1})	41.60
$F(000)$	632
θ range (deg)	3.33–28.5
Index ranges	$-10 \leqslant h \leqslant 10$, $0 \leqslant k \leqslant 15$, $-7 \leqslant l \leqslant 7$
Reflections collected [$I > 2\sigma(I)$]	1944
Independent reflections [$I > 2\sigma(I)$]	1013 [$R(int) = 0.056$]
Refinement method	Full-matrix least-squares on F^2
Data/restraints/parameters	1013/74
Goodness of fit on F^2	1.185
Final R indices [$I > 2\sigma(I)$]	$R_1 = 0.0255$, w$R_2 = 0.0447$
Extinction coefficient	0.051(1)
Largest diff. peak and hole (e Å^{-3})	4.07 (0.03 Å from Bi) and −3.50 (0.67 from Bi)

3.2. Resolution of the structure

The resolution of the structure of $BiMgVO_5$ has been done from single crystal X-ray diffraction data collected at room temperature. The unit cell dimensions were determined and refined with a least squares fit of 1944 reflections with $I > 2\sigma(I)$ and $3.33° < \theta < 28.47°$. The refinement was performed with SHELXL-93 [14]. The structure was solved by the heavy atom method and refined in the monoclinic space group $P2_1/n$. Atomic coordinates of the bismuth atom were determined from the Patterson map. The position of Mg, V and O atoms were deduced from subsequent refinements and analyses of difference electron density maps. The maximum residual electron density was near the Bi atoms. A summary of the crystal data for $BiMgVO_5$ is given in Table 1. Final atomic coordinates, and thermal parameters are listed in Tables 3 and 4, respectively. Selected bond distances and bond angles are given in Table 5.

3.3. Structural description of $BiMgVO_5$

The structure of $BiMgVO_5$ (Fig. 2) is similar to that of BiMPO$_5$ (M = Mn, Co, Ni) [4,6,7]. It is formed by

Table 2
X-ray powder diffraction data of $BiMgVO_5$

$2\theta_{obs}$	$100I/I_0$	d_{obs}	h	k	l	$2\theta_{cal}-2\theta_{obs}$
14.459	20	6.121	1	1	0	0.003
15.248	39	5.806	0	2	0	−0.004
18.157	75	4.882	1	0	−1	0.002
19.116	48	4.639	0	1	−1	−0.001
19.625	69	4.520	1	2	0	−0.002
23.298	17	3.815	0	2	1	−0.001
23.791	10	3.737	1	2	−1	0.002
24.306	4	3.659	1	0	1	0.003
24.710	9	3.600	2	0	0	−0.002
25.502	67	3.490	1	1	1	0.004
25.879	24	3.440	2	1	0	0.009
26.111	7	3.410	1	3	0	0.000
26.848	3	3.318	2	1	−1	0.005
29.150	47	3.061	2	2	0	0.010
29.425	14	3.033	1	3	−1	−0.004
30.023	100	2.974	2	2	−1	0.006
30.775	32	2.903	0	4	0	−0.008
33.255	29	2.692	1	4	0	−0.013
33.679	64	2.659	1	3	1	−0.001
33.969	26	2.637	2	3	0	0.007
34.729	37	2.581	1	1	−2	0.006
35.452	27	2.530	2	1	1	0.015
35.966	24	2.495	1	4	−1	−0.009
36.282	22	2.474	0	1	2	0.028
36.806	4	2.440	2	0	−2	−0.011
37.621	11	2.389	2	1	−2	0.007
38.252	41	2.351	3	1	0	0.008
39.564	17	2.276	3	2	−1	0.014
40.510	36	2.2250	2	4	−1	0.007
41.286	8	2.1850	1	3	−2	0.001
41.928	24	2.1530	1	1	2	−0.008
42.803	29	2.1110	0	5	1	−0.003
43.385	8	2.0840	3	3	−1	−0.002
43.827	10	2.0640	2	3	−2	−0.015
44.370	39	2.0400	3	3	0	0.001
46.359	22	1.9570	3	2	−2	0.010
47.072	24	1.9290	2	5	−1	0.003
48.294	6	1.8830	3	4	−1	0.008
49.015	9	1.8570	4	1	−1	−0.037
49.786	14	1.8300	3	3	−2	−0.030
52.358	35	1.7460	1	5	−2	0.003
52.847	27	1.7310	4	0	−2	0.007
53.480	17	1.7120	4	1	−2	0.004
53.717	10	1.7050	2	6	0	0.001
54.267	8	1.6890	3	4	−2	−0.032
54.972	15	1.6690	3	5	0	−0.008
56.291	7	1.6330	4	3	0	0.026
56.783	16	1.6200	0	2	3	0.006
57.402	11	1.6040	1	3	−3	−0.027
57.796	8	1.5940	1	5	2	−0.001
58.316	10	1.5810	4	3	−2	0.037
58.479	10	1.5770	0	7	1	0.013
59.897	12	1.5430	1	0	3	−0.011
61.032	10	1.5170	2	6	−2	0.014
61.300	10	1.5110	1	7	1	−0.005
61.708	19	1.5020	4	2	1	−0.004
61.982	14	1.4960	5	1	−1	−0.003
64.982	13	1.4340	1	3	3	0.022

Sys.: monoclinique; S.G.: $P2_1/n$ $(Z=4)$, $a=7.5439(7)$ Å, $b=11.615(2)$ Å, $c=5.3017(7)$ Å, $\beta=107.35(1)°$, $V=443.4(1)$ Å^3, $M(20)=107.8$; $F(30)=102.7(0.0063, 46)$.

Table 3
Atomic coordinates and equivalent isotropic displacement parameters ($Å^2\times10^4$) for $BiMgVO_5$

Atom	x	y	z	U_{eq}
Bi	0.18168(3)	0.09245(2)	0.11105(4)	72(2)
Mg	0.8224(3)	0.0808(2)	0.3751(4)	86(4)
V	0.0249(2)	0.3506(1)	0.2176(2)	59(2)
O(1)	0.3244(6)	0.9308(4)	0.0301(8)	105(8)
O(2)	−0.0163(6)	0.2161(4)	0.3174(8)	133(8)
O(3)	0.8247(7)	0.4266(4)	0.0857(8)	133(9)
O(4)	0.4822(5)	0.4742(4)	0.2472(7)	75(8)
O(5)	0.6256(6)	0.1730(4)	0.4788(8)	138(9)

Table 4
Anisotropic displacement parameters ($Å^2\times10^4$) for $BiMgVO_5$

Atom	U_{11}	U_{22}	U_{33}	U_{23}	U_{13}	U_{12}
Bi	81(2)	63(2)	80(2)	3(1)	36(1)	−8(1)
Mg	103(10)	84(10)	87(9)	−5(7)	50(8)	−8(8)
V	64(4)	51(4)	71(4)	−4(4)	34(3)	0(4)
O(1)	136(20)	108(18)	85(17)	−18(15)	53(15)	0(20)
O(2)	128(19)	120(19)	169(19)	0(17)	71(16)	12(20)
O(3)	138(21)	132(19)	118(18)	−48(16)	22(16)	14(20)
O(4)	92(18)	78(18)	68(15)	13(14)	42(14)	9(17)
O(5)	190(22)	117(20)	161(19)	−12(16)	137(17)	7(20)

The anistropic displacement factor exponent takes the form: $-2\pi^2[h^2a^{*2}U_{11}+\cdots+2hka^*b^*U_{12}]$.

Table 5
Bond distances (Å) and angles (deg) for $BiMgVO_5$

Bond distances		Angles	
Bi–O(4)#1	2.129(4)	Mg#2–O(4)–Bi#10	107.5(2)
Bi–O(4)#2	2.203(4)	Mg#2–O(4)–Mg#11	98.3(2)
Bi–O(1)#3	2.268(4)	Bi#10–O(4)–Mg#11	104.8(2)
Bi–O(3)#4	2.435(4)	Mg#2–O(4)–Bi#6	140.6(2)
Bi–O(2)	2.543(4)	Bi#10–O(4)–Bi#6	103.5(2)
Bi–O(5)#2	2.814(4)	Mg#11–O(4)–Bi#6	96.6(2)
Mg–O(5)	2.035(5)	O(5)#2–V–O(3)#9	108.6(2)
Mg–O(2)#5	2.065(5)	O(5)#2–V–O(2)	104.4(2)
Mg–O(4)#6	2.083(4)	O(3)#9–V–O(2)	112.3(2)
Mg–O(1)#7	2.108(4)	O(5)#2–V–O(1)#1	109.1(2)
Mg–O(3)#8	2.149(5)	O(3)#9–V–O(1)#1	109.4(2)
Mg–O(4)#8	2.167(4)	O(2)–V–O(1)#1	112.8(2)
O(4)–Mg#2	2.083(4)		
O(4)–Bi#10	2.129(4)		
O(4)–Mg#11	2.168(4)		
O(4)–Bi#6	2.203(4)		
V–O(5)#2	1.682(4)		
V–O(3)#9	1.708(5)		
V–O(2)	1.708(4)		
V–O(1)#1	1.745(4)		

Note. Symmetry transformations used to generate equivalent atoms: #1, $-x+1/2$, $y-1/2$, $-z+1/2$; #2, $x-1/2$, $-y+1/2$, $z-1/2$; #3, x, $y-1$, z; #4, $x-1/2$, $-y+1/2$, $z+1/2$; #5, $x+1$, y, z; #6, $x+1/2$, $-y+1/2$, $z+1/2$; #7, $-x+1$, $-y+1$, $-z$; #8, $-x+3/2$, $y-1/2$, $-z+1/2$; #9, $x-1$, y, z; #10, $-x+1/2$, $y+1/2$, $-z+1/2$; #11, $-x+3/2$, $y+1/2$, $-z+1/2$.

$[Mg_2O_{10}]$, $[Bi_2O_{10}]$ and VO_4 groups (Fig. 3). The $[Mg_2O_{10}]$ dimer is based on two MgO_6 octahedra sharing an edge. The $[Bi_2O_{10}]$ dimer is formed by two much distorted BiO_6 octahedra sharing an edge. The structure can also be described as a tridimensional network of $[Mg_2O_{10}]$ dimers linked by VO_4 tetrahedra; this forms large tunnels along *c*-axis where Bi^{3+} are located (Fig. 4).

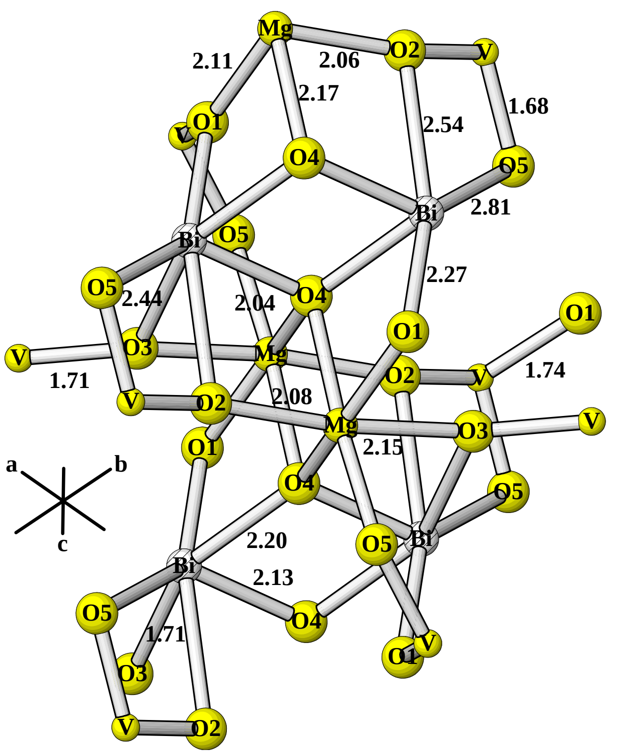

Fig. 2. Atom connections in the $BiMgVO_5$ crystal structure.

3.3.1. Magnesium atoms

The Mg atom is coordinated to six oxygen atoms which form octahedron with bond distances ranging from 2.035 to 2.167 Å. These values are close to the ionic radii sum (2.12 Å) of Mg^{2+} and O^{2-} [13]. Two MgO_6 share one common edge (O_4–O_4) and form $[Mg_2O_{10}]$ dimer (Fig. 3) with Mg–Mg distance of 3.21 Å. The other corners O_1, O_2, O_3 and O_5 are connected to VO_4 tetrahedra.

3.3.2. Bismuth atoms

The Bi atom is coordinated to six oxygen atoms with bond distances ranging from 2.203 to 2.814 Å, the sum of the ionic radii is 2.42 Å. Every BiO_6 polyhedron is connected to another BiO_6 by common edge (O_4–O_4) (Fig. 3) and to three VO_4 tetrahedra: one by common edge (O_2–O_5) and two others by corners O_1 and O_3. Bi–Bi distance is 3.40 Å.

3.3.3. Vanadium atoms

The VO_4 tetrahedron shares its four corners with four different $[Mg_2O_{10}]$ units, and two corners with two different $[Bi_2O_{10}]$ units and one edge (O_2–O_5) with one $[Bi_2O_{10}]$ unit. V–O distances vary from 1.682 to 1.745 Å and are inferior to the calculated value 1.76 Å from Shannon table [13]. OVO angles vary from 104.4° to 112.8°. The VO_4 tetrahedra are slightly distorted due to the corner and edge-sharing between the VO_4 unit and $[M_2O_{10}]$ dimeric unit.

3.3.4. Oxygen atoms

The O_1, O_2, O_3 and O_5 atoms are bonded to Bi, V, and Mg. The O_4 atom participates only to Mg–Mg and Bi–Bi dimers. As the O_4 oxygen does not bond to (VO_4)

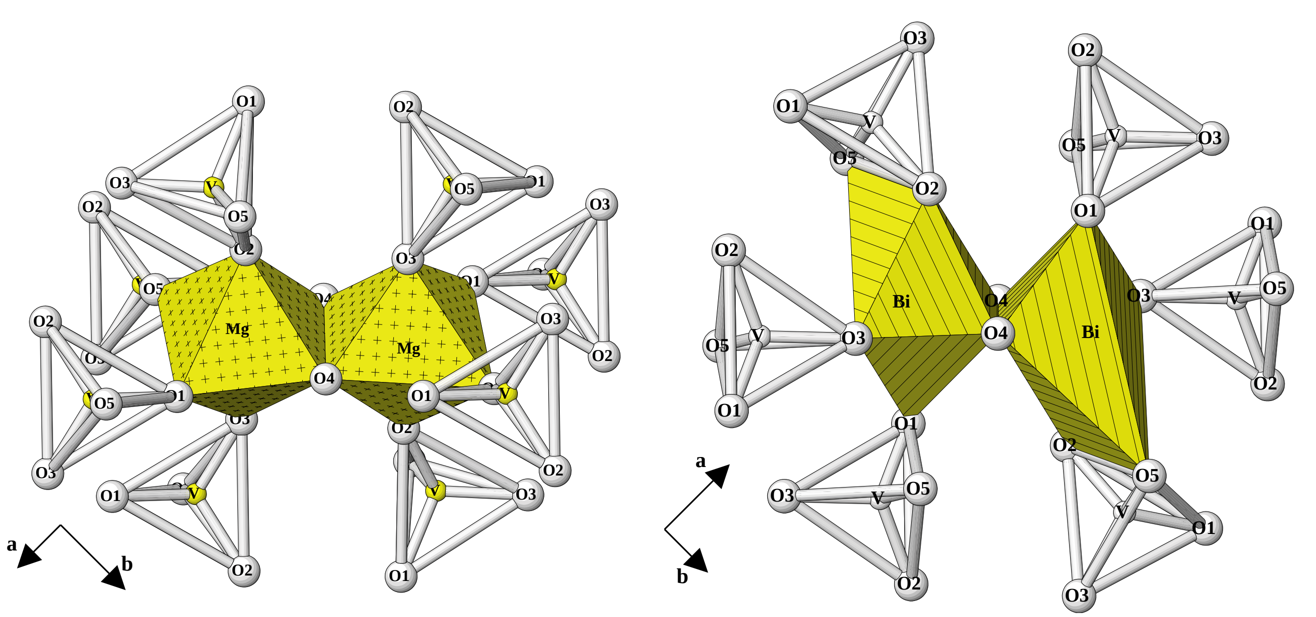

Fig. 3. $[M_2O_{10}]$ (M = Mg, Bi) dimers and VO_4 tetrahedra.

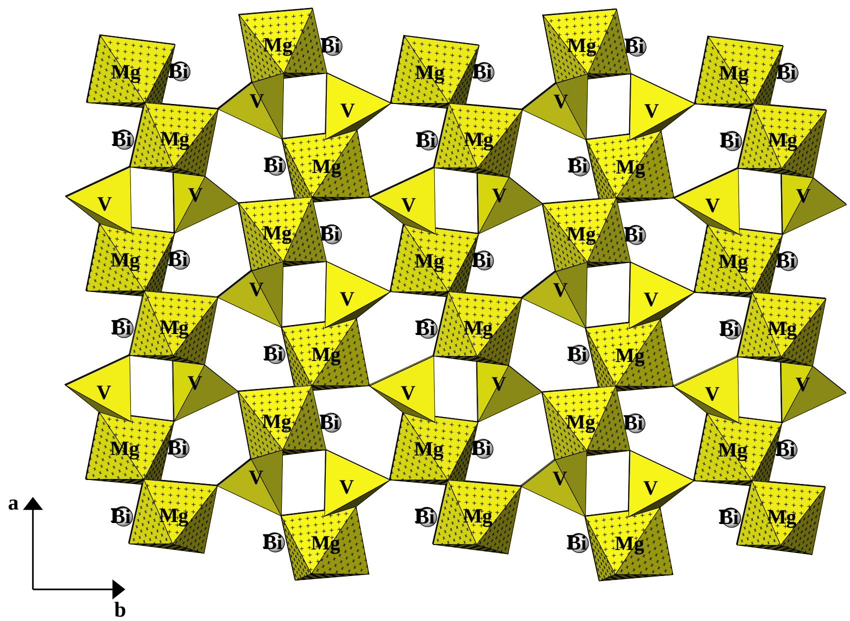

Fig. 4. Projection of the $BiMgVO_5$ structure along the *c*-axis.

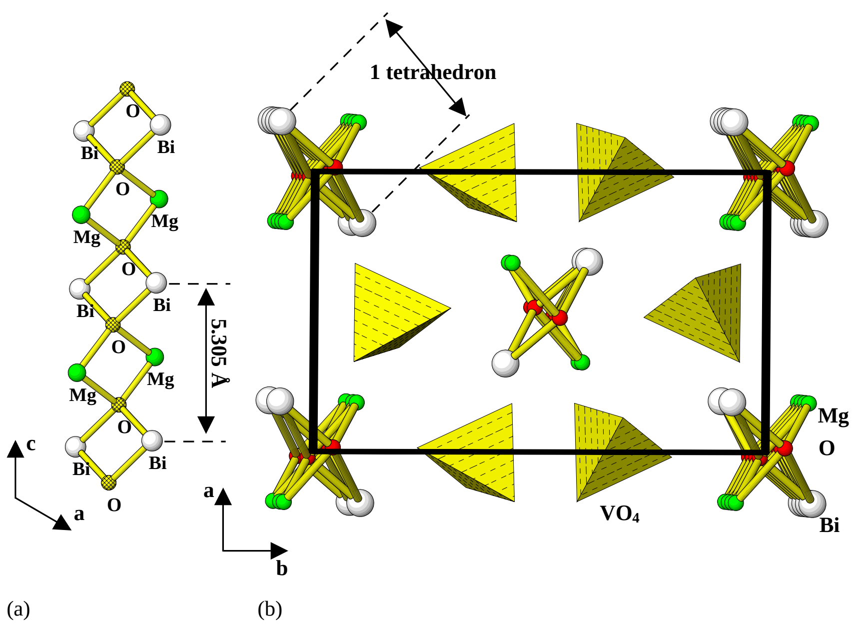

Fig. 5. (a) The one tetrahedron large mono-dimensional chain in $BiMgVO_5$ compounds running along *c*-axis of the monoclinic unit cell and (b) the crystal structure viewed along [001] direction showing the arrangement of $(OBiMg)^{3+}$ chains and VO_4^{3-} groups.

group, the title compound is an oxyvanadate: $BiMgO(VO_4)$.

Recently, Abraham and coworkers [15] have proposed a new description of the structure of bismuth transition metal oxyphosphates privileging the tetrahedral cationic environment of oxygen atoms not bounded to P^{5+} ion. The structure of $BiMgO(VO_4)$ can be regarded as a file of edge-shared OBi_2Mg_2 tetrahedra running along *c* direction. The OBi_2Mg_2 tetrahedra share opposite Bi–Bi and Mg–Mg edges constituting a file of composition $(OBiMg)^{3+}$.The $(VO_4)^{3-}$ tetrahedra are inserted between the cationic files as shown in Fig. 5.

They extend this new concept to numerous structures characterized by oxy anions (oxyphosphates, oxyvanadates, oxysulfates) [16]. The cationic tetrahedra can be a chain, a column, and a layer depending of the stoichiometry.

Bond valence sums, $S_i = \sum_j \exp(R_{ij} - d_{ij})/b$ with $b = 0.37$ Å [17], are in good agreement with the expected formal oxidation states of Bi^{3+}, Mg^{2+}, V^{5+} and O^{2-} ions (Table 6).

3.4. Vibrational spectroscopy

An analysis of the infrared and Raman vibrations reveals a total of $24A_g+24B_g+24A_u+24B_u$ lattice modes which can be expected for the $BiMgVO_5$ crystal, including the acoustical modes A_u+B_u. Table 7 shows the origin, as well as a summary of the infrared and Raman activity, of the modes. Vibrational analysis for an isolated VO_4^{3-} point group Td leads to 4 modes: $A_1[(\nu_1:\nu_s(VO_4)]$, $E[(\nu_2:\delta_s(VO_4)]$ and $2F_2[\nu_3:\nu_{as}(VO_4)$ and ν_4: $\delta_{as}(VO_4)]$. All of these are Raman active whereas only ν_3 and ν_4 are infrared active. In $BiMgVO_5$ the vanadium atom is in a C_1 symmetry site; therefore, we expect under the factor group 8 Raman-active modes for the stretching vibrations: $\nu_1(A_g,B_g)+3\nu_3\ (A_g,B_g)$ and 8 IR-active modes: $\nu_1(A_u,B_u)+3\nu_3(A_u,B_u)$. For the bending vibrations we achieved 10 Raman-active modes: $2\nu_2(A_g,B_g)+3\nu_4(A_g,B_g)$ and 10 IR-active modes: $2\nu_2(A_u,B_u)+3\nu_4(A_u,B_u)$. The external modes consist of the translational vibrations of the Mg^{2+}, Bi^{3+} and VO_4^{3-} ions. Fig. 6 shows Raman and infrared spectra of $BiMgVO_5$. The high frequency part (700–1000 cm^{-1}) of the Raman spectrum corresponds to the internal stretching vibrations of the VO_4 tetrahedra and exhibits 3 bands (852, 805, 748 cm^{-1}), the predicted ones are eight. In this region of the infrared spectrum 7 bands (1040, 1019, 978, 864, 837, 819, 768 cm^{-1}) are observed. For the V–O bending vibrations, four Raman bands (570, 389, 340, 303 cm^{-1}) were observed, the predicted ones are ten and in the infrared spectrum 8 bands (550, 523, 507, 442, 423, 384, 359, 311 cm^{-1}) are observed. The bands observed in the 300–700 cm^{-1} region may be due also to the vibrations of Bi–O bonds. The bands in the lower frequency region, 150–300 cm^{-1}, are attributed to the external modes.

Hardcastle and Wachs [18] have proposed and tested for vanadium compounds the equation for the correlation between the Raman stretching vibration of V–O bond and bond length d_{V-O}: $\nu = 21349\ \exp(-1.9176 d_{V-O})$. We have applied this relation to $BiMg_2VO_6$ [19], $BiVO_4$, $GdVO_4$ [20] and $BiMgVO_5$. The results reported in Table 8 show that the values of V–O distances estimated from Raman data are

Table 6
Bond valence calculations for $BiMgVO_5$

	Bi	Mg	V	V_i	V_{theo}
O(1)	0.62	0.32	1.17	2.11	2
O(2)	0.29	0.36	1.29	1.94	2
O(3)	0.39	0.29	1.29	1.97	2
O(4)	0.90	0.35		2.27	2
O(4)	0.74	0.28			
O(5)	0.14	0.40	1.39	1.93	2
V_i	3.08	2.00	5.14		
V_{theo}	3	2	5		

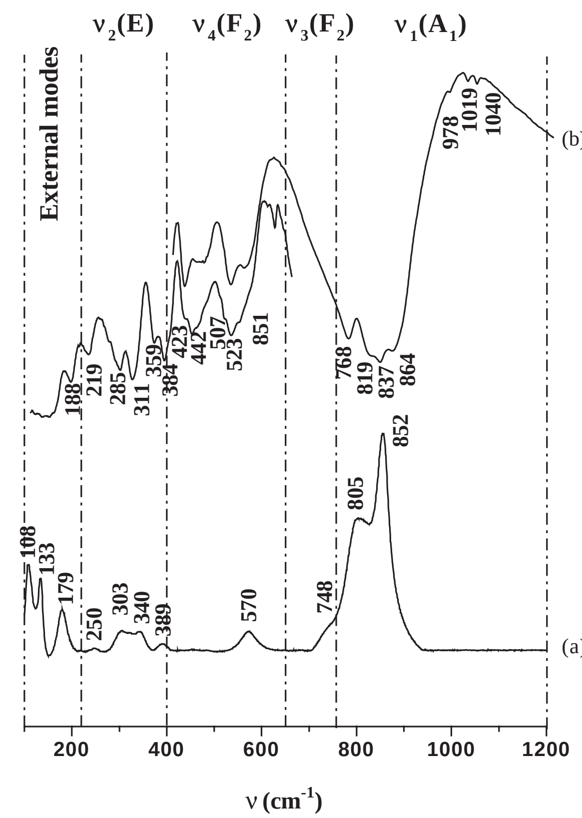

Fig. 6. Raman (a) and infrared (b) spectra of $BiMgVO_5$.

Table 7
A summary of the lattice vibrations and its origin in crystalline $BiMgVO_5$

Activity	$C_{1\Rightarrow C_2h}$	$\ni_V$	$\ni_{Bi}$	$\ni_{Mg}$	$\ni_O$	Total irreducible representation of crystal, $\ni_{crystal}$	Acoustical vibrations, $\ni_{acoustic}$	Lattice vibrations in $BiMgVO_5$, $\ni_{vibrations}$
R	A_g	3	3	3	15	24	0	24
R	B_g	3	3	3	15	24	0	24
IR	A_u	3	3	3	15	24	1	23
IR	B_u	3	3	3	15	24	1	23

Table 8
Comparison of V–O bond lengths obtained from X-ray diffraction and Raman

Compound	Stretches ν (cm^{-1})	Bond lengths d_{V-O} (Å)		
		Raman	X-ray diffraction	Ref.
$BiVO_4$	$\nu_1(A_1) = 824$	1.697		
	$\nu_1(A_1) = 874$	1.666	$V–O \times 4 = 1.727$	[20]
	$\nu_3(F_2) = 708$	1.776		
$GdVO_4$	$\nu_1(A_1) = 882$	1.662		
	$\nu_1(A_1) = 823$	1.697	$V–O \times 4 = 1.664$	[20]
	$\nu_3(F_2) = 808$	1.707		
$BiMg_2VO_6$	$\nu_1(A_1) = 911$	1.645		
	$\nu_1(A_1) = 864$	1.672	$V–O \times 2 = 1.672$	[19]
	$\nu_3(F_2) = 773$	1.730	$V–O \times 2 = 1.725$	
$BiMgVO_5$	$\nu_1(A_1) = 852$	1.679	$V–O \times 1 = 1.682$	This work
	$\nu_1(A_1) = 805$	1.709	$V–O \times 2 = 1.708$	
	$\nu_3(F_2) = 748$	1.747	$V–O \times 1 = 1.745$	

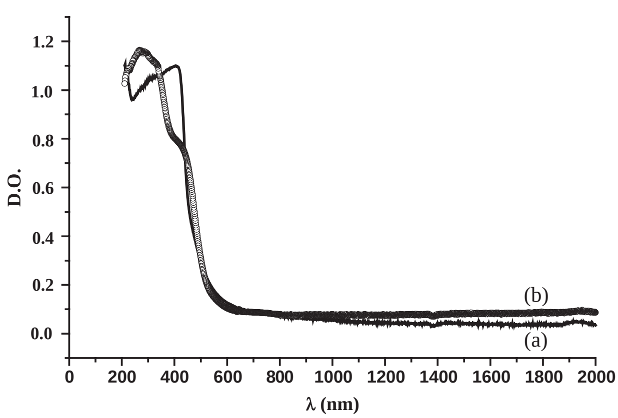

Fig. 7. Diffuse reflection spectra of Bi_2O_3 (a) and $BiMgVO_5$ (b).

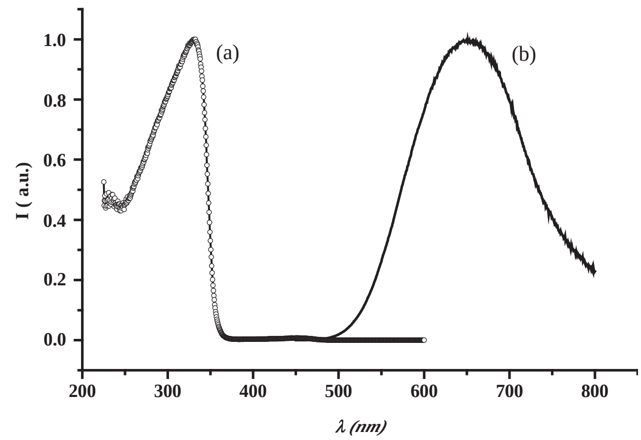

Fig. 8. Excitation ($\lambda_{em} = 640$ nm) (a) and emission ($\lambda_{exc} = 343$ nm) (b) of the $BiMgVO_5$ luminescence at 7 K.

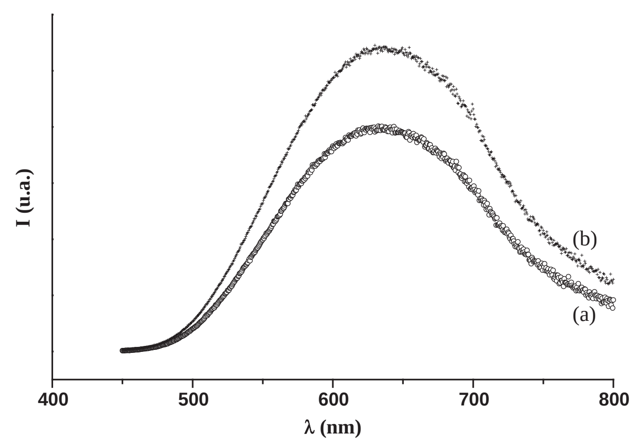

Fig. 9. Emission spectra of $BiMgVO_5$ at $T = 292$ K (a) $\lambda_{exc.} = 343$ nm; (b) $\lambda_{exc.} = 350$ nm.

in good agreement with those obtained from X-ray diffraction.

3.5. Optical properties

The diffuse reflectance spectrum of $BiMgVO_5$ (Fig. 7) powder exhibits at room temperature absorption bands at 400 and 280 nm. The absorption may be due to different transitions of Bi^{3+} ion, O–Bi charge transfer and O–V charge transfer as observed in YPO_4:Bi^{3+} at 230 nm ($^1S_0 \rightarrow {}^3P_1$ transition) [21] in Bi_2O_3 at 400 nm (O–Bi CT) [22] and in YVO_4 at 300 nm (O–V CT) [23].

For excitation at shorter wavelengths (254 nm or 343 nm) than the absorption edges, at 7 K, an intense broad-band emission is observed extending from 500 to 800 nm and peaking at 653 and 651 nm, respectively (Figs. 8 and 9). This emission is also observed at room temperature with a shift toward high energy (633 nm for $\lambda_{exc} = 343$ nm) with a decrease by 10 of intensity, relative to a low thermal quenching. The excitation spectrum shows a band between 250 and 380 nm with maximum at 340 nm (Fig. 8). The Stokes shift is about 12340 cm^{-1} at 7 K.

Luminescence in pure vanadates and in Bi^{3+} doped vanadates has been previously reported (Table 9). The emission of the Bi^{3+} and the VO_4^{3-} group consists of broad bands extending in a wide spectral region.

When excited by UV radiations in the wavelength range 315–360 nm, YVO_4 and $Mg_3(VO_4)_2$ show luminescence with an emission band in all the visible domain, peaking at 420 and 570 nm, respectively [23]. These emissions are attributed to charge transfer transitions in VO_4^{3-} ions.

YVO_4:Bi^{3+} which has been extensively studied [24,25] shows a broad emission band extending from 400 to 700 nm with a maximum at 567 nm under UV radiation excitation at 254 and 365 nm. It was demonstrated in the (Bi,Y)VO_4 system that the emission and the absorption shifts to longer wavelengths for higher concentrations of Bi. An emission band around 650 nm was reported for

Table 9
Some data on the luminescence of vanadium and bismuth compounds

Compound	Center	Optical absorption edge (nm) (at 300 K)	Excitation maximum (nm)	Emission maximum (nm)	Ref.
YVO_4	V^{5+}		314	420	[23]
$Mg_3(VO_4)_2$	V^{5+}		315	570	[23]
$BiCaVO_5$	Bi^{3+}/V^{5+}	360	330	560	[26]
YVO_4:Bi	Bi^{3+}/V^{5+}		340	567	[24,25]
$BiMgV_2O_6$	Bi^{3+}/V^{5+}		450	650	[19]
$BiMgVO_5$	Bi^{3+}/V^{5+}	340	343	651	This work

$BiMg_2VO_6$ [19]. $BiCaVO_5$ shows at 4.2 K an efficient yellow emission with a maximum at 540 nm [26].

The red emission observed in $BiMgVO_5$ at 651 nm can be attributed to Bi^{3+} and/or $(VO_4)^{3-}$ with a possible charge transfer between these ions. The more valuable hypothesis is to attribute emission to Bi^{3+} with the existence of energy transfer from the matrix $(VO_4)^{3-}$ ions to the emitting centers Bi^{3+}.

The observed difference in emission wavelength of bismuth vanadate compounds is probably due to the difference in crystal structure. (Bi, Y)VO_4 zircon-type structure is built of alternating edge sharing VO_4 tetrahedra and (Bi, Y)O_8 bisdisphenoids extending parallel to *c* direction and joined laterally by edge-sharing bisdisphenoids forming zigzag chains parallel to *a*-axis. $BiMg_2VO_6$ and $BiCaVO_5$ structures are characterized by $(BiO_2)^-$ chains whereas as described before in $BiMgVO_5$ Bi atoms constitute Bi_2O_{10} dimers. The connection of vanadium tetrahedra are nearly the same in these compounds. Isolated $(VO_4)^{3-}$ tetrahedron shares edge and corners with three Bi polyhedra belonging to three $(BiO_2)^-$ chains in $BiCaVO_5$ and edge and corners with three Bi polyhedra of three different Bi dimers in $BiMgVO_5$.

More precise optical characterization including decay times are under work in order to confirm the proposed attribution.

4. Conclusion

Powder and single crystals of $BiMgVO_5$ have been prepared. Its crystal structure has been resolved in $P2_1/n$ space group. It is formed by a 3D network of $[Mg_2O_{10}]$ dimers connected by VO_4 tetrahedra. This forms large tunnels occupied by Bi^{3+} ions. Vibrational spectra are reported. V–O bond lengths have been calculated from Raman assignment and are in good agreement with those obtained from X-ray diffraction. An intense red emission is observed between 500 and 800 nm peaking at 651 nm at 7 K.

Acknowledgment

The authors would like to thank E. Lebraud for his help in crystal selection.

References

[1] T. Takahashi, H. Iwahara, Mater. Res. Bull. 13 (1978) 1447.
[2] F. Abraham, M.F. Debreuille-Gresse, G. Mairesse, G. Nowogrocki, Solid State Ionics 28–30 (1988) 529.
[3] S. Uma, R. Bliesner, A.W. Sleight, Solid State Sci. 4 (2002) 329–333.
[4] F. Abraham, M. Ketatni, Eur. J. Solid State Inorg. Chem. 32 (1995) 429–437.
[5] S. Nadir, J.S.S. Winnea, H. Steinfink, J. Solid State Chem. 148 (1999) 295–301.
[6] M. Ketatni, F. Abraham, O. Mentre, Solid State Sci. 1 (1999) 449–460.
[7] M. Ketatni, O. Mentre, F. Abraham, Philos. Res. Bull. 10 (1999) 160–165.
[8] X. Xun, S. Uma, A. Yokochi, A.W. Sleight, J. Alloys Compd. 338 (2002) 51–53.
[9] J. Boje, Hk. Muller-Buschbaum, Z. Anorg. Allg. Chem. 619 (1993) 521–524.
[10] X. Xun, A. Yokochi, A.W. Sleight, J. Solid State Chem. 168 (2002) 224–228.
[11] I. Radosavljevic, J.A.K. Howard, A.W. Sleight, Int. J. Inorg. Mater. 2 (2000) 543–550.
[12] L.H. Brixner, C.M. Foris, Mater. Res. Bull. 9 (1974) 273–276.
[13] R.D. Shannon, C.T. Prewitt, Acta Crystallogr. B 25 (1969) 925.
[14] G.M. Sheldrick, Shelxl-93 Program Refinement of Crystal Structure, Institut Anorganische Chemie, Göttingen, Germany, 1993.
[15] F. Abraham, O. Cousin, O. Mentre, El.M. Ketnani, J. Solid State Chem. 167 (2002) 168–181.
[16] S. Giraud, A. Mizrahi, M. Drache, P. Conflant, J.P. Wignacourt, H. Steinfink, Solid State Sci. 3 (2001) 593–602.
[17] N.E. Brese, M. O'Keeffe, Acta Crystallogr. B 47 (1991) 192–197.
[18] F.D. Hardcastle, I.E. Wachs, J. Phys. Chem. 95 (1991) 5031–5041.
[19] J. Huang, A.W. Sleight, J. Solid State Chem. 100 (1992) 170–178.
[20] A. Lorriaux-Rubbens, J. Corset, J. Ghamri, H. Baussart, Adv. Mater. Res. 1–2 (1994) 433–446.
[21] G. Blasse, A. Bril, J. Chem. Phys. 48 (1968) 217.
[22] V. Dolocan, F. Iova, Phys. Stat. Sol. A 64 (1981) 755–759.
[23] H. Ronde, G. Blasse, J. Inorg. Nucl. Chem. 40 (1978) 215–219.
[24] R.K. Datta, J. Electrochem. Soc. Solid State Sci. 114 (10) (1967) 1057–1063.
[25] R. Moncorgé, G. Boulon, J. Luminescence 18–19 (1979) 376–380.
[26] Z. Pei, A. van Dijken, A. Vink, G. Blasse, J. Alloys Compd. 204 (1994) 243–246.